Exploring the Interior of Hollow Fluorescent Carbon Nanoparticles

ARTICLE *in* THE JOURNAL OF PHYSICAL CHEMISTRY C · FEBRUARY 2013

Impact Factor: 4.77 · DOI: 10.1021/jp311252v

5 AUTHORS, INCLUDING:

Tarasankar Das
Indian Institute of Science Education and Res…
20 PUBLICATIONS **73** CITATIONS
SEE PROFILE

Arnab Maity
Indian Institute of Science Education and Res…
22 PUBLICATIONS **74** CITATIONS
SEE PROFILE

Pradipta Purkayastha
Indian Institute of Science Education and Res…
73 PUBLICATIONS **819** CITATIONS
SEE PROFILE

THE JOURNAL OF PHYSICAL CHEMISTRY C

Article

pubs.acs.org/JPCC

Exploring the Interior of Hollow Fluorescent Carbon Nanoparticles

Somen Mondal, Tarasankar Das, Prasun Ghosh, Arnab Maity, and Pradipta Purkayastha*

Department of Chemical Sciences, Indian Institute of Science Education and Research, Kolkata, Mohanpur Campus, Mohanpur 741252, WB, India

Supporting Information

ABSTRACT: We synthesized hollow fluorescent carbon nanoparticles (HFCNs) using the simple procedure reported by Fang et al. [*ACS Nano* **2012**, *6*, 400−409]. The size distribution was uniform, providing spherical carbon nanoparticles with a hollow. In the present work we have focused on exploration of the interior of the HFCNs as this was hardly clarified until now. Understanding the importance of HFCNs in biological aspects due to their potentially low cytotoxicity and inherent fluorescent property, we have defined that the polarity of the interior of the HFCNs resembles that of ethanol by using suitable hydrophobic and hydrophilic fluorescent probes. Moreover, we have shown that π-electron-rich hydrophobic molecules, such as pyrene, can form a $\pi-\pi$ stack with the inner wall of the HFCNs. Our findings are expected to open avenues in the usage of HFCNs as drug carriers and markers in bioimaging.

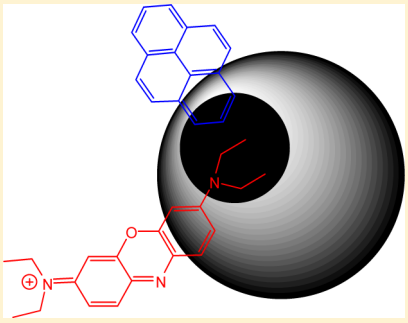

INTRODUCTION

Fluorescent nanoparticles have been the center of semiconductor and bioimaging research for quite some time now. One of the fields where much interest is shown has been the semiconductor quantum dots (QDs). These devices have attracted much recent attention for their potential uses as optical imaging materials.[1−4] However, a widely accepted fact about QDs containing cadmium or other heavy metals is toxicity. Even low concentrations of the QDs can be appreciably toxic for biological systems.[5−7] Cadmium and selenium are the principal components of the majority of QDs. These metals are known to be acutely and chronically toxic to cells and organisms as they get accumulated in the cellular calcium membrane channels.[8,9] Cadmium inhibits the synthesis of DNA, RNA, and proteins.[10,11]

In search for nontoxic alternative QD-like fluorescent nanomaterials, it is recently found that small carbon nanoparticles could be surface-passivated by organic or biomolecules to become strongly fluorescent in the visible and near-infrared spectral regions.[12] These surface-functionalized carbon nanoparticles (CNs) are physicochemically and photochemically stable and nonblinking.[12−14] Most CNs are excited in between 330 and 420 nm and emit in the wavelength range of 400−600 nm depending on the size.[15] Carbon is generally a nontoxic element and hardly comes under the same category as cadmium and other heavy metals. Various routes for preparation of CNs have been reported.[16−20] From high degree of complexities down to extremely simple methods have been proposed to synthesize the CNs. Among the popular methods, mention can be made of microwave pyrolysis of glucose[21] and ultrasonic irradiation of glucose.[16] Simple processes such as oxidation of candle soot to prepare CNs have been attempted.[18,19] Depending on a specific application area, various methods have been applied for synthesis of CNs with different structures and morphologies.[22−25] Silica template has been used to prepare CNs with ordered pore structure for the application to catalysis and electrochemistry.[24−26] Polymer as porogen to prepare porous carbon is another efficient method. Reaction-induced phase separation of miscible polymer blends have been applied in recent past to prepare nanostructure carbonaceous material with continuous pores.[27,28] Recently, carbon particles with microporous shell and mesoporous core were prepared through internal phase separation within the droplets of an oil-in-water emulsion.[29]

In attempts for better and simplified synthetic techniques to prepare hollow carbon nanoparticles (HCNs), a few methods came up that produce excellent size distribution for the HCNs.[30,31] A self-assembly approach using hexachlorobenzene and sodium (Na) had been adopted to obtain 50−100 nm HCNs.[30] Preparation of hollow fluorescent carbon nanoparticles (HFCNs) with green emission has been reported very recently.[31] Simple mixing of acetic acid, water, and diphosphorus pentoxide produced the desired HFCNs. In comparison to traditional dyes and quantum dots, HFCNs are claimed to be superior fluorescent bioimaging agents because of their low toxicity, stability, and resistance to photobleaching.

The relatively large fraction of void space in hollow structures has been regularly used to encapsulate and control release of drugs, sub-nanoparticles, and DNA. The void space in hollow particles has been used to modulate optical properties, increase active area for catalysis, etc. To make use of the full significance of HFCNs since they are practically nontoxic to biological systems, in addition to the methods of synthesis one needs to know about the characteristics of their

Received: November 14, 2012
Revised: January 30, 2013
Published: February 7, 2013

   dx.doi.org/10.1021/jp311252v | *J. Phys. Chem. C* 2013, 117, 4260−4267

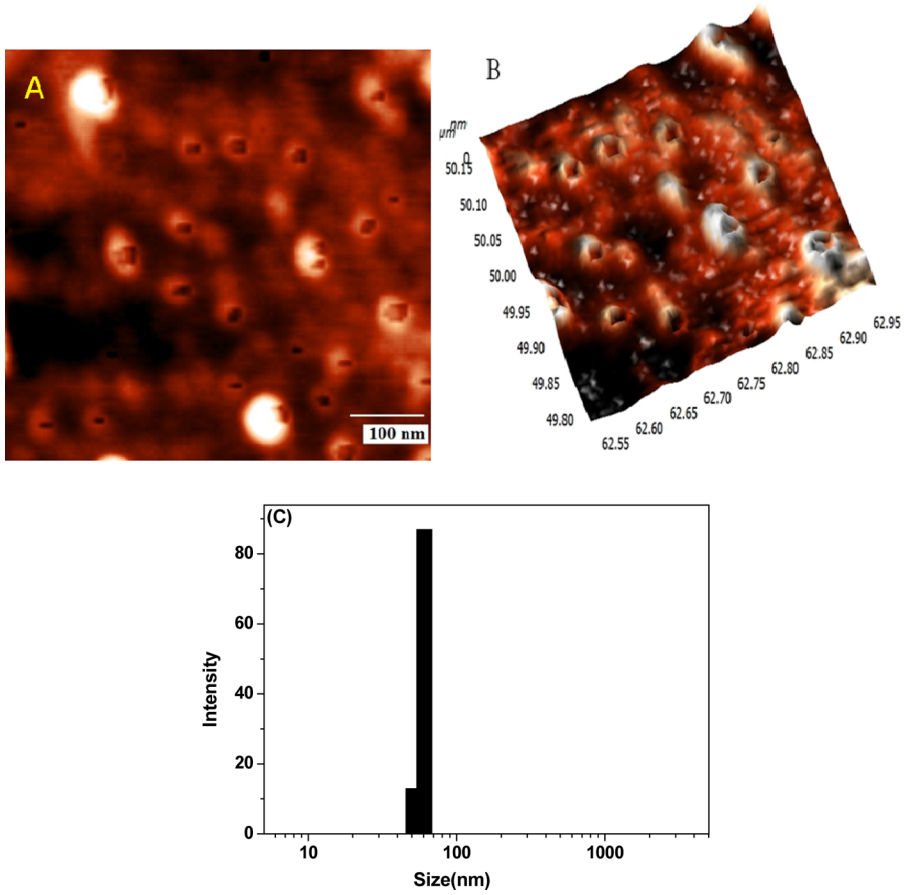

Figure 1. 2D and 3D AFM images of HFCNs (A, B). (C) Average size distribution of HFCNs in water obtained by DLS analysis.

interior. This lacunae in the studies of HFCNs has been highlighted in the present article, and different molecular probes have been used to explore the interior of the HFCNs. Keeping in mind that the HFCNs have a graphitic surface, we used pyrene (Py) which supposedly adheres to the internal surface of the hollow vessels because of hydrophobic effect and $\pi-\pi$ interaction. To monitor the internal polarity, we have adopted oxazine-725 (Ox-725) as a probe.

MATERIALS AND METHODS

Materials. Glacial acetic acid, diphosphorus pentoxide, ethyl acetate, sodium hydroxide, carbon black, nitric acid, and ethylenediamine were purchased from Sigma-Aldrich. Triple distilled water was used for the preparation of the experimental solutions.

Preparation of HFCN. HFCN has been prepared following a previously reported simple procedure.[31] Briefly, a mixture of acetic acid (AC) and water was added to diphosphorus pentoxide (P_2O_5) in a beaker without stirring and kept it for cooling for 10 min. A brown sticky liquid was obtained, which was dispersed in water. Finally, the HFCNs were extracted with ethyl acetate, and the pH was adjusted to 7.

Each of the three precursors (AC, water, and P_2O_5) played a very important role in the self-catalytic reaction to produce the HFCNs. AC was particularly selected as the carbon precursor. The water in the medium liberated heat from the system; i.e., the reaction was exothermic. On the other hand, the dehydrating agent P_2O_5 accelerated the carbonization reaction.[31]

Preparation of Solid Fluorescent Carbon Nanoparticle (SFCN). A mixture of carbon black and aqueous nitric acid (5 M) was refluxed for 12 h. This was followed by centrifugation at 8000 rpm, and the supernatant was collected. Ethylenediamine was added to the supernatant for surface passivation and refluxed at 110 °C for 3 days under nitrogen atmosphere. A yellow solution was obtained, which was centrifuged at 10 000 rpm for 10 min, and the supernatant was collected for further use.[32]

Spectral Measurements. The absorption spectra were recorded using a Varian Cary 300 Bio UV−vis spectrophotometer. Fluorescence measurements were made using a PerkinElmer LS 55 scanning spectrofluorimeter. The fluorescence lifetimes were measured by the method of time-correlated single-photon counting using a picoseconds spectrofluorimeter from HORIBA Jobin Yvon IBH. The instrument was equipped with a FluoroHub single photon counting controller and a FC-MCP-50SC MCP-PMT detection unit. Either a laser head or a nano-LED pulsed diode powered by a pulsed diode controller (IBH) was used as the excitation light source. The excitation wavelengths used were 377, 340, 405, and 635 nm as per the cases. The typical detection time of these was 70 ps. To calculate the lifetime, the fluorescence decay curves were analyzed by an iterative fitting program provided by IBH. Atomic force microscopic studies for characterization were performed using an NT-MDT NTEGRA instrument procured from NT-MDT (Santa Clara, CA). Sizes of the CNs were measured by dynamic light scattering (DLS) using a Malvern Zetasizer Nano equipped with a 4.0 mW HeNe laser operating at λ = 633 nm. All samples were measured in an

dx.doi.org/10.1021/jp311252v | J. Phys. Chem. C 2013, 117, 4260−4267

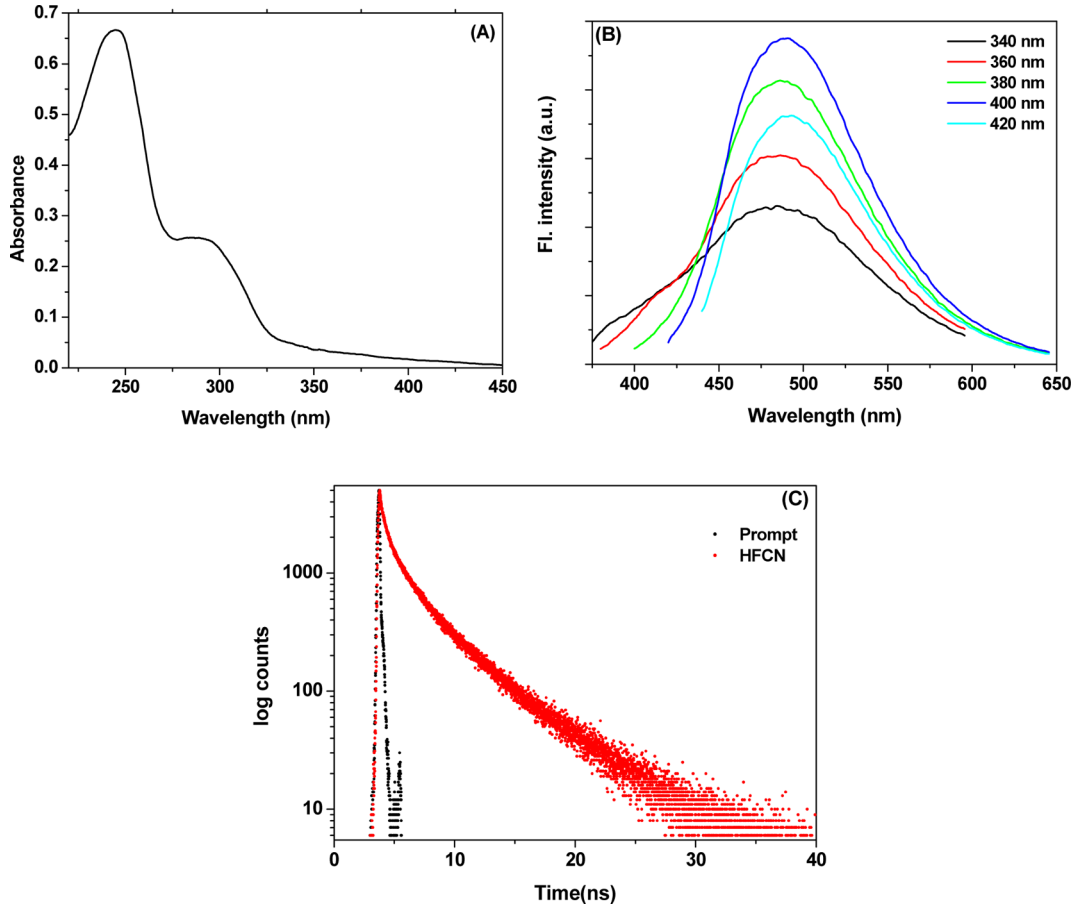

Figure 2. (A) Absorption spectrum, (B) steady-state fluorescent spectra, and (C) time-resolved fluorescence decay of HFCN (λ_{ex} = 377 nm, λ_{em} = 490 nm).

aqueous medium at room temperature with a scattering angle of 173°. The size distribution was calculated by Nano x software using a non-negative least-squares analysis (NNLS).

Characterization of HFCN. AFM images of the HFCNs are shown in Figure 1A,B. The hollow core and the vessel nature of the HFCNs are clearly visible. The thickness of the carbon shell is about 5 nm.[31] DLS experiment shows that the average particle size of the HFCNs is in the range 60−70 nm (Figure 1C) and also that they are monodispersed. Monodispersity is optimal for biomedical applications.

The HFCNs were further characterized by UV−vis spectroscopy. The absorption spectrum shows two bands at 245 and 297 nm (Figure 2A). The band at 245 nm is likely to originate due to the formation of multiple polyaromatic chromophores, while the broad peak at 297 nm may be attributed to the n−π* transitions in C═O on the HFCNs.[31,32] The carbon source with carboxylic group (AC) introduces oxygenous defects in the CNs that impose the fluorescence property. Furthermore, the polyaromatic structure may serve as fluorescent chromophore that makes HFCN a fluorophore.[31] Figure 2B shows emission spectra of HFCN on excitations from 340 to 420 nm. The emission maximum practically has no shift as the excitation wavelength is varied. This indicates that there is a uniform distribution of size for the HFCNs. The characteristic luminescence decay for the HFCNs is found to be biexponential (Figure 2C) with decay times 2.42 ns (81%) and 360 ps (18%).

RESULTS AND DISCUSSION

Potential applications of HFCNs in different aspects of biomedical backgrounds emerge out directly due to their characteristic fluorescent property. Where SFCNs can act as very useful biomarkers and have sufficient potential to replace robust systems, such as QDs, HFCNs carry the additional benefit of acting as a carrier for useful small molecules. Their capacity for encapsulating sensitive materials such as therapeutics, fluorescent markers, and field-responsive agents are proven facts for drug delivery and biomedical imaging. To understand these promising carriers better, in the present work we have ventured to explore their internal environment. To do this, we have selected few small molecules that have been used as systems with a purpose. Simple pyrene is one of the probes that are used because of its unique molecular characteristics.

Pyrene (Py) is well-known to be a hydrophobic molecule and a probe that is extremely sensitive to polarity of the medium.[33,34] It has a typical characteristic feature to form excimers in polar environment whereas to remain as monomers in lower polarity.[35,36] Like the normal hosts for small molecule guests, the interior of the HFCNs can be anticipated to be of lower polarity compared to the bulk aqueous medium. Under this circumstance one can measure the parameters of the microenvironment inside the HFCNs by using satellite probes that are prone to the hydrophobic cavity. Remembering that Py exists preferably as monomers in lower polarity and excimer in higher polarity, we employed this probe to interact with the HFCNs. Absorbance of Py gets decreased (Figure 3A) and the

dx.doi.org/10.1021/jp311252v | J. Phys. Chem. C 2013, 117, 4260−4267

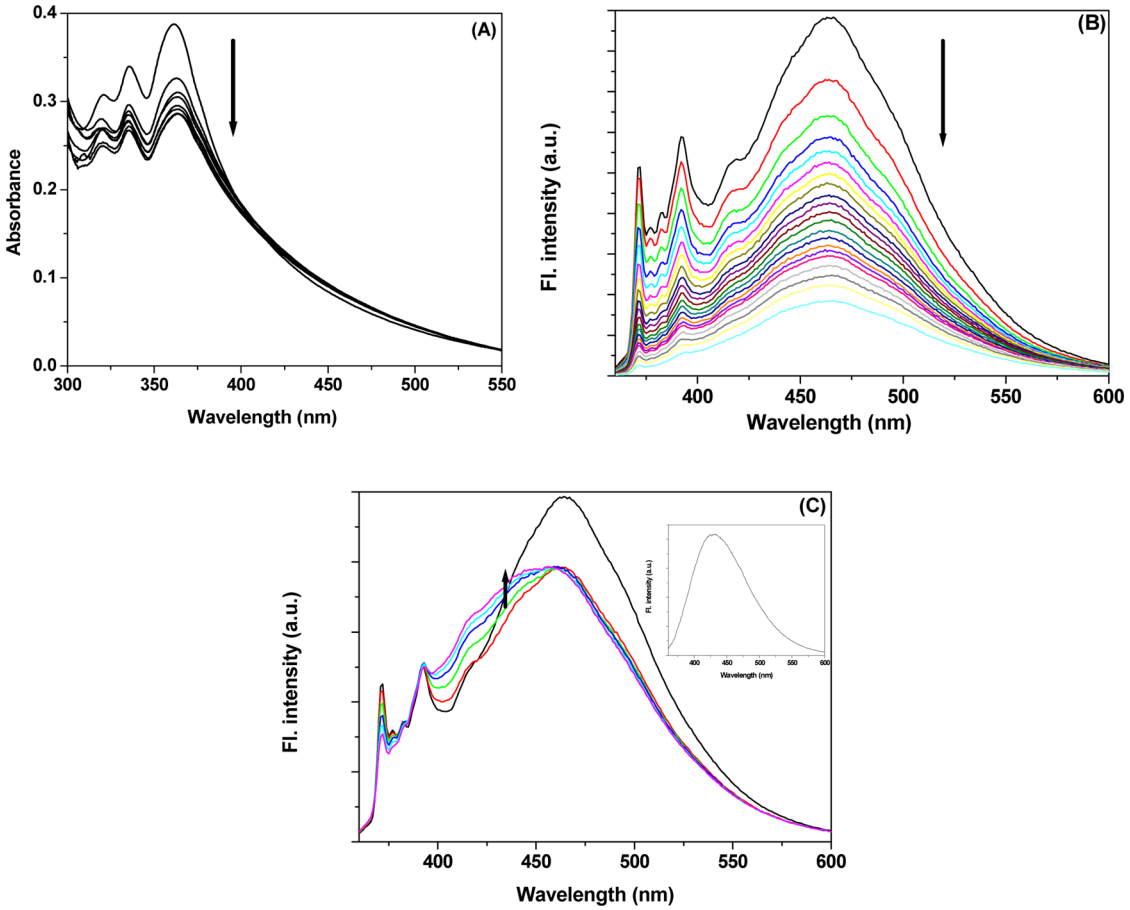

Figure 3. (A) Absorption spectra and (B) steady-state fluorescent spectra of Py with increase in HFCN concentration. (C) Fluorescence emission of Py in presence of gradually enhanced concentration of SFCN (λ_{ex} = 340 nm). Inset of (C) shows the emission spectrum of SFCN in water; the fluorescence spectrum of Py in water is indicated by the black trace. There was an initial quenching of Py fluorescence on addition of SFCN, after which no further change in fluorescence intensity is observed. Enhancement in emission intensity at ~430 nm (as indicated by the arrow in (C)) is due to the addition of SFCN to the Py solution.

Table 1. Time-Resolved Fluorescence Decay Data for Py Monomer in the Absence and Presence of HFCN[a]

	τ_1 (ns)	% contribution	τ_2 (ns)	% contribution	τ_3 (ps)	% contribution	χ^2
pyrene	5.5	7	18.0	62	349	31	1.10
pyrene with periodic addition of HFCN	3.13	8	16.2	62	386	30	1.15
	1.71	12	14.7	58	323	29	1.09
	1.49	15	14.1	53	297	31	1.12
	1.07	21	12.8	47	168	30	1.16

[a] χ^2 signifies the appropriateness of the fit to the raw data. The sample was excited with a 340 nm radiation and monitored at 390 nm. The raw decay data are shown in Figure S2 of the Supporting Information.

fluorescence emissions from both Py monomer and excimer were found to get remarkably quenched with an increase in the concentration of HFCNs in solution (Figure 3B). While comparing with change in fluorescence of Py on interaction with solid FCNs (SFCNs) (Figure 3C), we found that the profuse quenching of Py fluorescence is unique to the HFCNs.

As mentioned earlier that Py tends to exist as monomer in lower polarity, we could expect a conversion of the Py excimer to monomer if the molecules enter inside the cavity of the HFCN. The vibronic structures (peaks I and III) of Py emission are extremely sensitive to the polarity of the environment, and the peak ratio is routinely used to determine the micropolarity of the medium. This peak ratio can be qualitatively taken as a measure of the extent of interaction between the Py system and the solvents of different polarities. Traditionally, a value above 1.5 is an indication of Py experiencing a hydrophilic environment, whereas a value of 0.6 suggests a hydrophobic milieu.[37−39] Considering our data from the change in fluorescence of Py due to interaction with HFCN, the ratio between the intensities of peak I (I_1, ~371 nm) and peak III (I_3, ~382 nm) comes to be 1.18. This dictates that the polarity of the interior of the HFCNs resembles that of ethanol.[40] It is known that excimer formation does not take place at micromolar concentration of Py (typically 6 μM in our experiment).[41]

However, at reduced polarity, as inside the interior of HFCN, existence of pyrene excimer will be minimized. Thus, the π-electron-rich pyrene monomers may get docked to the interior π-electron-rich wall of the HFCN through $\pi-\pi$ stacking interaction. We have verified this by performing steady-state

dx.doi.org/10.1021/jp311252v | J. Phys. Chem. C 2013, 117, 4260−4267

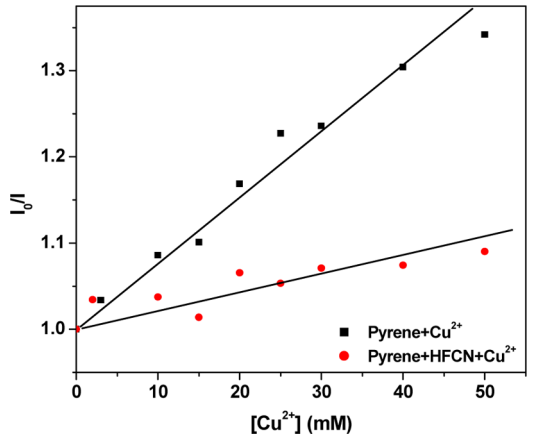

Figure 4. Plot of relative fluorescence intensity of Py monomer (monitored at 390 nm) against concentration of Cu^{2+}. I_0 indicates the fluorescence intensity without the quencher ion, and I signifies the intensities at different rising concentrations of Cu^{2+}.

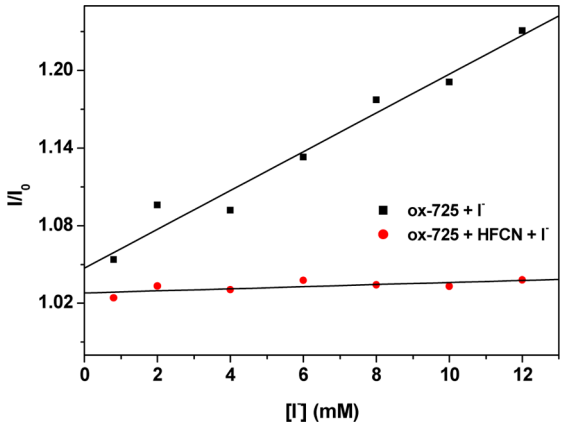

Figure 6. Plot of relative fluorescence intensity of ox-725 monomer (monitored at 670 nm) against concentration of I^-. I_0 indicates the fluorescence intensity without the quencher ion, and I signifies the intensities at different rising concentrations of I^-.

anisotropy experiment monitoring the pyrene monomer and the excimer emissions with increase in HFCN concentration. The anisotropy (r) increases considerably for the pyrene monomer, whereas it did not change significantly for the excimer (see Figure S1 in Supporting Information). Hence, the internal polarity for HFCN provided by pyrene monomers is not supposed to be the exact value since, due to the stacking with the internal wall of the HFCN, the probe molecule will give it rotational freedom to experience the actual environment.

Conversion of Py excimer to monomer inside the HFCNs leads to quenching of the fluorescence emission from the former as is observed in Figure 3B. Arguably, we see a quenching of the monomer emission as well along with the excimer. As is known that the CNs have graphene-like walls with extensive π-electron cloud,[31] the possibility of $\pi-\pi$

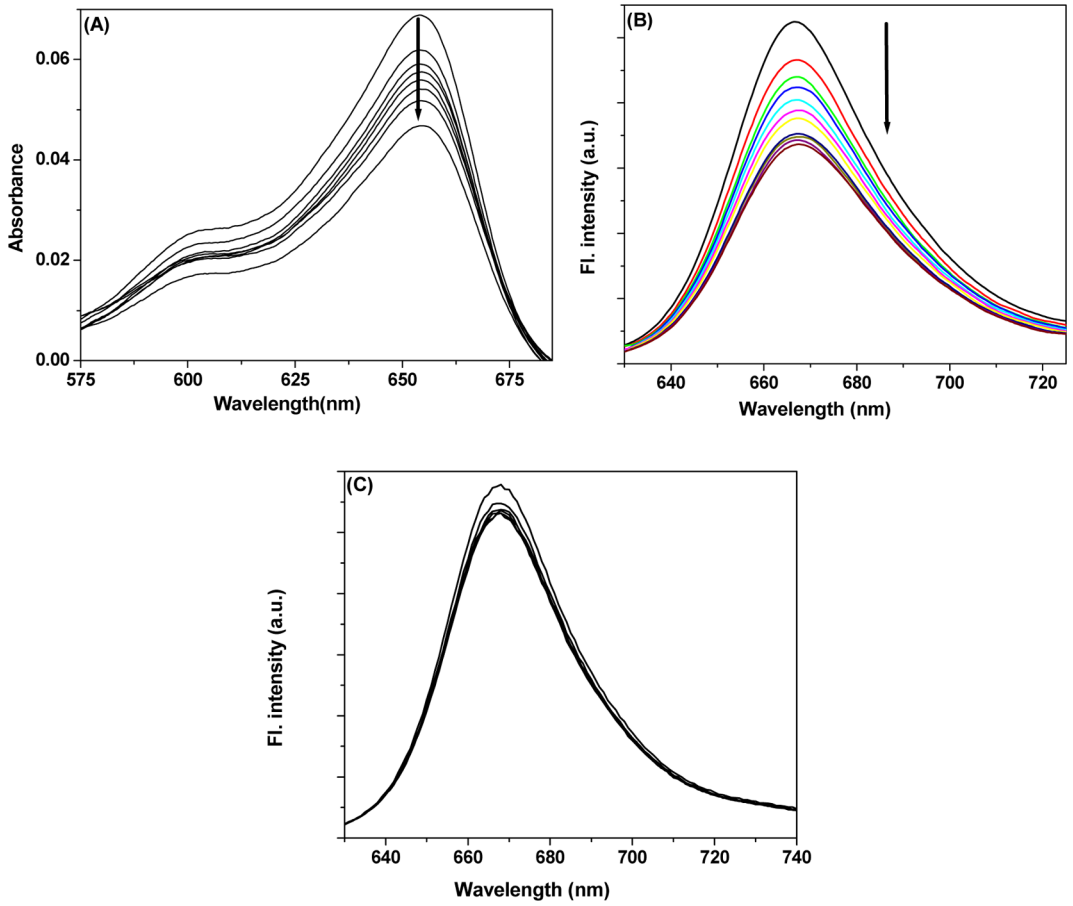

Figure 5. (A) Absorption spectra and (B) steady-state fluorescent spectra of ox-725 with increase in HFCN concentration. (C) Fluorescence emission of ox-725 in the presence of gradually enhanced concentration of SFCN (λ_{ex} = 630 nm).

dx.doi.org/10.1021/jp311252v | J. Phys. Chem. C 2013, 117, 4260−4267

Table 2. Time-Resolved Fluorescence Decay Data for ox-725 in the Absence and Presence of HFCN[a]

	τ_1 (ps)	% contribution	τ_2 (ps)	% contribution	χ^2
Ox-725	496	100			1.18
Ox-725 with periodic addition of HFCN	446	77.0	667	22.3	0.98
	433	75.3	716	24.6	0.98
	436	74.6	747	25.3	1.02
	440	75.3	823	24.6	1.01

[a] χ^2 signifies the appropriateness of the fit to the raw data. The sample was excited with a 635 nm radiation and monitored at 670 nm. The raw decay data are shown in Figure S3 of the Supporting Information.

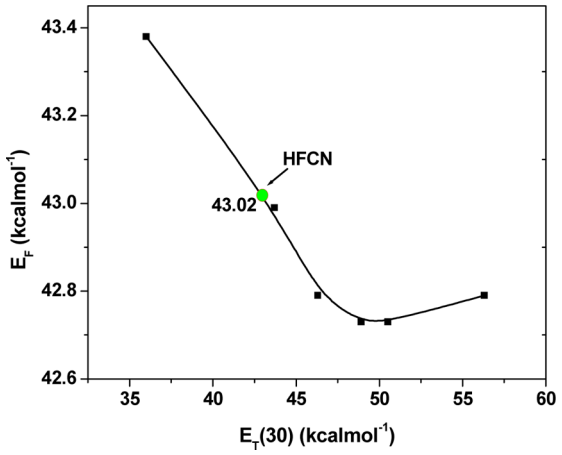

Figure 7. Plot of fluorescence energy (E_F) obtained from the maxima of the emissions from ox-725 dissolved in dioxane–water mixtures with different ratios of the two solvents against $E_T(30)$ values of the solvent mixtures. The green dot in the plot shows the $E_T(30)$ value of the interior of the HFCNs.

interaction between the Py monomers inside the cavity with the inner walls of the HFCNs cannot be ignored. This phenomenon, in turn, may lead to quenching of the fluorescence of the Py monomers due to energy transfer as reflected in Figure 3B. Thus, unlike the previous studies on simple incorporation of Py inside cavities and release,[39] we propose that for an electron-rich system, such as Py monomer, it is possible that the species cling to the inside of the vessels with graphene-like walls. In a recent study, Matte et al. have shown that graphene can quench fluorescence of organic donor molecules, such as pyrenebutanoic acid succinimidyl ester through photoinduced electron transfer.[42] Fluorescence decay of Py could be fitted to a three-component decay. Photoinduced electron transfer results to significant decrease in all the three components.[42] We have observed a very similar phenomenon on interaction of Py with HFCN as shown in Table 1.

The incorporation of Py inside the HFCNs has been further evidenced by employing Cu^{2+} ions as quenchers to the Py monomer emission. Cu^{2+} quenches Py fluorescence much more in bulk water than that in presence of a certain concentration of HFCN (Figure 4). The calculated Stern–Volmer constants determining the extent of quenching in the two cases are 7.08 and 1.5 M^{-1}, respectively. The quenching efficiencies by Cu^{2+} in free and encapsulated systems indicate that pyrene is indeed inside the HFCNs.[43]

Since the HFCNs fluoresce at ~500 nm, the Py excimer emission overlaps with it, and also as discussed above, Py monomers get adhered to the inner walls of the HFCNs. Although we could get the characteristics about the polarity of the interior of the HFCNs by employing Py as a probe, we opted for another probe, oxazine 725 (ox-725). Ox-725 is a cationic dye and has been used here in lieu of the negative surface charge of the HFCNs due to the presence of the carboxylic groups.

The absorption spectral changes in case of ox-725 are similar to that we observed for Py. The absorbance decreased on addition of HFCNs to the solution (Figure 5A). The fluorescence of the dye got somewhat quenched by the HFCNs (Figure 5B), indicating a change in the environment of the dye molecules. This is verified by doing a control experiment using ox-725 and SFCNs, where there is practically no change in fluorescence intensity of ox-725 due to the SFCNs (Figure 5C). Because of the positive charge on the dye molecule, the negatively charged HFCNs will attract them, reinforcing the ox-725 molecules to approach the HFCNs and enter the interior. However, the emission maximum of ox-725 does not show any shift due to the polarity of the medium. Thus, to verify the encapsulation of the dye molecules, we examined the ability of quenching of fluorescence of ox-725 by I^- (Figure 6). The Stern–Volmer quenching constants obtained thus for ox-725 in the absence and presence of the HFCNs are 15.3 and 7.8 M^{-1}, respectively, which indicates ox-725 entrapment inside the HFCN cavities.

The entrapment of ox-725 inside the HFCNs has been further evidenced by time-resolved fluorescence decay measurements (Table 2). The probe shows a single component decay profile in bulk water environment, whereas in the presence of HFCNs a second faster component evolves out. The latter picoseconds component is evidently due to the HFCN-ox-725 composite.

Using ox-725 as a probe, we have redetermined the internal polarity of the HFCNs. The probe was dissolved in dioxane–water mixtures bearing different polarities. The plot of fluorescence energies (E_F) against $E_T(30)$ yields the internal polarity of HFCN to be ~43.02, showing that the HFCN interior is even less polar than ethanol/methanol (see Figure S4 in Supporting Information and Figure 7).[44] This looks realistic because unlike pyrene, ox-725 will not dock to the internal wall of HFCN and thus should produce the actual polarity of the interior.

■ CONCLUSIONS

In summary, we have been able to report precisely about the internal environment of hollow fluorescent carbon nanoparticles. FCNs have been recognized to be extremely useful for bioimaging due to their photostability and noncytotoxicity. HFCNs carry the significance several steps ahead as they can carry drugs to the sites specified. We have used a recent reported technique to synthesize the HFCNs.[31] Since there is not much in the literature about the characteristics of the interior of HFCNs, it becomes inevitable to explore this area to apply these biocompatible agents in drug delivery and bioimaging. Using the electron-rich pyrene probe, cationic dye oxazine-725, we have shown that the HFCNs can serve as useful shelter for compounds with parametric differences. Pyrene can form π–π stack with the inner graphene-like wall of the HFCNs. The negatively charged surface of the HFCNs can attract cationic probes to encapsulate. Our report shows that

dx.doi.org/10.1021/jp311252v | J. Phys. Chem. C 2013, 117, 4260–4267

the interior of the HFCNs resembles a comparatively less polar environment than water which suits various biological events, especially protein folding.[45−47]

■ ASSOCIATED CONTENT

Supporting Information

Figures S1 and S2 demonstrating the raw data of fluorescence anisotropy and decay for Py, Figure S3 showing the fluorescence decay data for ox-725, and Figure S4 providing the fluorescence spectra of ox-725 in water−dioxane mixtures. This material is available free of charge via the Internet at http://pubs.acs.org.

■ AUTHOR INFORMATION

Corresponding Author

*E-mail: pradiptp@gmail.com.

Notes

The authors declare no competing financial interest.

■ ACKNOWLEDGMENTS

The work was supported by Department of Science and Technology, Government of India, through Project SR/S1/PC-35/2011. S.M. and A.M. acknowledge University Grants Commission, Government of India, and P.M. and T.D. are grateful to the Council of Scientific and Industrial Research, New Delhi, for their fellowships.

■ REFERENCES

(1) Medintz, I. L.; Uyeda, H. T.; Goldman, E. R.; Mattoussi, H. Quantum Dot Bioconjugates for Imaging, Labelling and Sensing. *Nat. Mater.* **2005**, *4*, 435−446.

(2) Xing, Y.; Rao, J. Quantum Dot Bioconjugates for in vitro Diagnostics & in Vivo Imaging. *Cancer Biomarkers* **2008**, *4*, 307−319.

(3) Morgan, N. Y.; English, S.; Wei, C.; Chernomordik, V.; Russo, A.; Smith, P. D.; Gandjbakhche, A. Real Time In Vivo Non-invasive Optical Imaging Using Near-infrared Fluorescent Quantum Dots. *Acad. Radiol.* **2005**, *12*, 313−323.

(4) Liu, H.; Zhang, X.; Xing, B.; Han, P.; Gambhir, S. S.; Cheng, Z. Radiation-Luminescence-Excited Quantum Dots for in vivo Multiplexed Optical Imaging. *Small* **2010**, *6*, 1087−1091.

(5) Derfus, A. M.; Chan, W. C. W.; Bhatia, S. N. Probing the Cytotoxicity of Semiconductor Quantum Dots. *Nano Lett.* **2004**, *4*, 11−18.

(6) Kirchner, C.; Liedl, T.; Kudera, S.; Pellegrino, T.; Javier, A. M.; Gaub, H. E.; Stolzle, S.; Fertig, N.; Parak, W. J. Cytotoxicity of Colloidal CdSe and CdSe/ZnS Nanoparticles. *Nano Lett.* **2005**, *5*, 331−338.

(7) Bottrill, M.; Green, M. Some Aspects of Quantum Dot Toxicity. *Chem. Commun.* **2011**, *47*, 7039−7050.

(8) Beyersmann, D.; Hechtenberg, S. Cadmium, Gene Regulation, and Cellular Signalling in Mammalian Cells. *Toxicol. Appl. Pharmacol.* **1997**, *144*, 247−261.

(9) Anas, A.; Akita, H.; Harashima, H.; Itoh, T.; Ishikawa, M.; Biju, V. Photosensitized Breakage and Damage of DNA by CdSe-ZnS Quantum Dots. *J. Phys. Chem. B* **2008**, *112*, 10005−10011.

(10) Stohs, S. J.; Bagchi, D. Oxidative Mechanisms in the Toxicity of Metal Ions. *Free Radical Biol. Med.* **1995**, *18*, 321−336.

(11) Prakash, S.; Rao, S.; Dameron, C. Cadmium Inhibits BPDE Alkylation of DNA in the Major Groove but Not in the Minor Groove. *Biochem. Biophys. Res. Commun.* **1998**, *244*, 198−203.

(12) Sun, Y.-P.; Zhou, B.; Lin, Y.; Wang, W.; Shiral Fernando, K. A.; Pathak, P.; Meziani, M. J.; Harruff, B. A.; Wang, X.; Wang, H.; Luo, P. G.; Yang, H.; Kose, M. E.; Chen, B.; Veca, L. M.; Xie, S.-Y. Quantum-Sized Carbon Dots for Bright and Colorful Photoluminescence. *J. Am. Chem. Soc.* **2006**, *128*, 7756−7757.

(13) Zhou, J.; Booker, C.; Li, R.; Zhou, X.; Sham, T.-K.; Sun, X.; Ding, Z. An Electrochemical Avenue to Blue Luminescent Nanocrystals from Multiwalled Carbon Nanotubes (MWCNTs). *J. Am. Chem. Soc.* **2007**, *129*, 744−745.

(14) Mochalin, V. N.; Gogotsi, Y. Wet Chemistry Route to Hydrophobic Blue Fluorescent Nanodiamond. *J. Am. Chem. Soc.* **2009**, *131*, 4594−4595.

(15) Xu, X.; Ray, R.; Gu, Y.; Ploehn, H. J.; Gearheart, L.; Raker, K.; Scrivens, W. A. Electrophoretic Analysis and Purification of Fluorescent Single-Walled Carbon Nanotube Fragments. *J. Am. Chem. Soc.* **2004**, *126*, 12736−12737.

(16) Li, H.; He, X.; Liu, Y.; Huang, H.; Lian, S.; Lee, T.; Kang, Z. One-step Ultrasonic Synthesis of Water-Soluble Carbon Nanoparticles with Excellent Photoluminescent Properties. *Carbon* **2011**, *49*, 605−609.

(17) Liu, C.; Zhang, P.; Tian, F.; Li, W.; Li, F.; Liu, W. One-Step Synthesis of Surface Passivated Carbon Nanodots by Microwave Assisted Pyrolysis for Enhanced Multicolor Photoluminescence and Bioimaging. *J. Mater. Chem.* **2011**, *21*, 13163−13167.

(18) Liu, H.; Ye, T.; Mao, C. Fluorescent Carbon Nanoparticles Derived from Candle Soot. *Angew. Chem., Int. Ed.* **2007**, *46*, 6473−6475.

(19) Tian, L.; Ghosh, D.; Chen, W.; Pradhan, S.; Chang, X.; Chen, S. Nanosized Carbon Particles From Natural Gas Soot. *Chem. Mater.* **2009**, *21*, 2803−2809.

(20) Wang, X.; Qu, K.; Xu, B.; Ren, J.; Qu, X. Microwave Assisted One-Step Green Synthesis of Cell-Permeable Multicolor Photoluminescent Carbon Dots without Surface Passivation Reagents. *J. Mater. Chem.* **2011**, *21*, 2445−2450.

(21) Zhu, H.; Wang, X.; Li, Y.; Wang, Z.; Yang, F.; Yang, X. Microwave Synthesis of Fluorescent Carbon Nanoparticles with Electrochemiluminescence Properties. *Chem. Commun.* **2009**, 5118−5120.

(22) Vander, R. L. Flame Synthesis of Ni-Catalyzed Nanofibers. *Carbon* **2002**, *40*, 2101−2107.

(23) Maser, W. K.; Benito, A. M.; Martinez, M. T. Production of Carbon Nanotubes: The Light Approach. *Carbon* **2002**, *40*, 1685−1695.

(24) Joo, S. H.; Choi, S. J.; Oh, I.; Kwak, J.; Liu, Z.; Terasaki, O.; Ryoo, R. Ordered Nanoporous Arrays of Carbon Supporting High Dispersions of Platinum Nanoparticles. *Nature* **2001**, *412*, 169−172.

(25) Kim, P.; Joo, J. B.; Kim, W.; Kang, S. K.; Song, I. K.; Yi, J. A Novel Method for the Fabrication of Ordered and Three Dimensionally Interconnected Macroporous Carbon with Mesoporosity. *Carbon* **2006**, *44*, 389−392.

(26) Joo, J. B.; Kim, P.; Kim, W.; Kim, J.; Kim, N. D.; Yi, J. Simple Preparation of Hollow Carbon Sphere via Templating Method. *Curr. Appl. Phys.* **2008**, *8*, 814−817.

(27) Yamazaki, M.; Teduka, M.; Ikeda, K.; Ichihara, S. Preparation of Carbon Materials with Coral-Like Continuous Pores Using Miscible Polymer Blends. *J. Mater. Chem.* **2003**, *13*, 975−977.

(28) Yamazaki, M.; Kayama, M.; Ikeda, K.; Alii, T.; Ichihara, S. Nanostructured Carbonaceous Material with Continuous Pores Obtained from Reaction-Induced Phase Separation of Miscible Polymer Blends. *Carbon* **2004**, *42*, 1641−1649.

(29) Jiang, Y. B.; Wei, L. H.; Yu, Y. Z.; Zhao, T. Preparation of Porous Carbon Particle with Shell/Core Structure. *Express Polym. Lett.* **2007**, *1*, 292−298.

(30) Hu, G.; Ma, D.; Cheng, M.; Liu, L.; Bao, X. Direct Synthesis of Uniform Hollow Carbon Spheres by a Self-Assembly Template Approach. *Chem. Commun.* **2002**, 1948−1949.

(31) Fang, Y.; Guo, S.; Li, D.; Zhu, C.; Ren, W.; Dong, S.; Wang, E. Easy Synthesis and Imaging Applications of Cross-Linked Green Fluorescent Hollow Carbon Nanoparticles. *ACS Nano* **2012**, *6*, 400−409.

(32) Ray, S. C.; Saha, A.; Jana, N. R.; Sarkar, R. Fluorescent Carbon Nanoparticles: Synthesis, Characterization, and Bioimaging Application. *J. Phys. Chem. C* **2009**, *113*, 18546−18551.

(33) Itoh, H.; Ishido, S.; Nomura, M.; Hayakawa, T.; Mitaku, S. Estimation of the Hydrophobicity in Microenvironments by Pyrene Fluorescence Measurements: n-β-Octylglucoside Micelles. *J. Phys. Chem.* **1996**, *100*, 9047−9053.
(34) Anthony, O.; Zana, R. Fluorescence Investigation of the Binding of Pyrene to Hydrophobic Microdomains in Aqueous Solutions of Polysoaps. *Macromolecules* **1994**, *27*, 3885−3891.
(35) Castanheira, E. M. S.; Martinho, J. M. G. Solvatochromic Shifts of Pyrene Excimer Fluorescence. *Chem. Phys. Lett.* **1991**, *185*, 319−323.
(36) Ghosh, P.; Mandal, S.; Das, T.; Maity, A.; Gupta, P.; Purkayastha, P. "Extra Stabilisation" of a Pyrene Based Molecular Couple by γ-Cyclodextrin in the Excited Electronic State. *Phys. Chem. Chem. Phys.* **2012**, *14*, 11500−11507.
(37) Kalyanasundaram, K.; Thomas, J. K. Environmental Effects on Vibronic Band Intensities in Pyrene Monomer Fluorescence and Their Application in Studies of Micellar Systems. *J. Am. Chem. Soc.* **1977**, *99*, 2039−2044.
(38) Winnik, F. M. Photophysics of Preassociated Pyrenes in Aqueous Polymer Solutions and in Other Organized Media. *Chem. Rev.* **1993**, *93*, 587−614.
(39) Kaushlendra, K.; Asha, S. K. Microstructural Reorganization and Cargo Release in Pyrene Urethane Methacrylate Random Copolymer Hollow Capsules. *Langmuir* **2012**, *28*, 12731−12743.
(40) Dong, D. C.; Winnik, M. The Py Scale of Solvent Polarities. *Can. J. Chem.* **1984**, *62*, 2560−2565.
(41) Parker, C. A.; Hatchard, C. G. Delayed Fluorescence of Pyrene in Ethanol. *Trans. Faraday Soc.* **1963**, *59*, 284−295.
(42) Matte, H. S. S. R.; Subrahmanyam, K. S.; Rao, K. V.; George, S. J.; Rao, C. N. R. Quenching of Fluorescence of Aromatic Molecules by Grapheme due to Electron Transfer. *Chem. Phys. Lett.* **2011**, *506*, 260−264.
(43) Makarova, O. V.; Ostafin, A. E.; Miyoshi, H.; Norris, J. R. Adsorption and Encapsulation of Fluorescent Probes in Nanoparticles. *J. Phys. Chem. B* **1999**, *103*, 9080−9084.
(44) Deng, Q.; Li, Y.; Wu, J.; Liu, Y.; Fang, G.; Wang, S.; Zhang, Y. Highly Sensitive Fluorescent Sensing for Water Based on poly(m-aminobenzoic acid). *Chem. Commun.* **2012**, *48*, 3009−3011.
(45) Pace, C. N.; Treviño, S.; Prabhakaran, E.; Scholtz, J. M. Protein Structure, Stability and Solubility in Water and Other Solvents. *Philos. Trans. R. Soc., B* **2004**, *359*, 1225−1235.
(46) Sasahara, K.; Nitta, K. Effect of Ethanol on Folding of Hen Egg-White Lysozyme Under Acidic Condition. *Proteins* **2006**, *63*, 127−135.
(47) Yang, Y.; Mayo, K. H. Alcohol-Induced Protein Folding Transitions in Platelet Factor 4: The O-State. *Biochemistry* **1993**, *32*, 8661−8671.